academicJournals

Vol. 8(37), pp. 929-952, 8 October, 2014
DOI: 10.5897/AJPP2014.4130
Article Number: 2A98DAC47895
ISSN 1996-0816

http://www.academicjournals.org/AJPP

African Journal of Pharmacy and Pharmacology

Full Length Research Paper

Projections of pharmacokinetic parameter estimates from mid-dose plasma concentrations in individuals on efavirenz: A novel approach

Tafireyi Nemaura

Department of Clinical Pharmacology, College of Health Sciences, University of Zimbabwe.

Received 23 June, 2014; Accepted 21 August, 2014

This work seeks to project individual pharmacokinetic (PK) parameter estimates of efavirenz (a drug with a long half life) from mid-dose concentrations and covariates, assuming full mass transfer of the drug. Gender, weight and CYP2B6, 516G>T genetic data of 61 patients on efavirenz containing highly active antiretroviral therapy (HAART) was collated and analysed. Models were derived to guide dose adjustment in patients predicted to have unsafe drug exposure, and new modelling methods and interpretations are suggested to estimate PK parameters. A new measure related to the uptake of the drug is incorporated in modelling of transportation (cumulative uptake volume). The cumulative uptake-volume associated with the full absorption of 600 mg of efavirenz was estimated to be 35.56 L whereas the volume of distribution was found to be 39.68 L. A sufficient relationship was established between estimated absolute oral bioavailability *(f)* and mid-dose concentration *(x)* at steady state $\{f = \frac{x^{1.121}}{x^{1.121}+3.135^{1.121}}, R^2 = 0.98\}$**. Patients who carry the CYP2B6 G516T TT genotype are projected to have high efavirenz exposure. The estimated bioavailability in this population ranges from (0.29; 0.86). Genotype, weight and gender based inference for dose adjustment proposition is evident for the drug efavirenz. The drug is projected to have been fully absorbed in 31 h in this population.**

Key words: Efavirenz, cumulative uptake-volume, bioavailability, volume of distribution, area under the curve (AUC), absorption rate.

INTRODUCTION

In addition to the enzyme CYP2B6, more studies have shown the potential role of other enzymes such as CYP2A6 and UGT 2B7 and drug transporters such as ABCB1 in efavirenz exposure levels (Habtewold et al., 2011;Mukonzo et al., 2009; Kwara et al., 2009; Ritchie et al., 2006). The study by Nyakutira et al. (2008) and those of others (Burger et al., 2006; Pedral-Sampaio et al., 2004; Mukonzo et al., 2009) observed a potential role of gender in efavirenz exposure levels. A study in Thailand observed that patient weight could also have an impact on exposure levels of efavirenz (Manosuthi et al., 2009). The pharmacokinetic (PK) and pharmacodynamic (PD)

*E-mail: tnemaura@gmail.com. Tel: +263776519990.

parameters of drugs used to treat human immuno-deficiency virus/acquired immune deficiency syndrome (HIV/AIDS) and/or tuberculosis (TB) have been shown to exhibit great inter-individual variability and interethnic variability (Friedland et al., 2006; Burger et al., 2006). Identifying subgroups occupying similar PK/PD clinical response space that requires modification of treatment strategy can greatly optimise the efficacy and safety in the use of current drugs.

Patient variability and changes occurring in the plasma concentrations affect the pharmacokinetics of efavirenz (Nyakutira et al., 2008; Sánchez et al., 2011). The differences in plasma concentrations are due to 'covariate' structure (in this work it is used as a variable that includes weight (W), genotype (CYP2B6 G516T) and gender (S)) and time. Weight, CYP2B6, and gender were considered the more likely covariates to influence efavirenz pharmacokinetics (Nyakutira et al., 2008; Rekić et al., 2011). The challenge then is to find a covariate structure that captures concentration differences. If one has relatively more information on the covariate structure that relates demographic, environmental and genetic factors to the dependent variable in this case concentration at mid-dose that is a strong correlation then a function can be formulated that relates the variables (Nemaura et al., 2012).

The time space has been used as the basis of the rate-defining variable in model formulation. In population pharmacokinetic modelling, covariates have been taken as additives and their inclusion into the structural model has commonly been investigated stepwise through backward/forward elimination regression methods (Ette and Williams, 2007). However, the developed covariate space is noted to be pivotal in the modelling and estimation of PK parameters in this work. It is used more importantly in the projection of bioavailability. The oral absorption of drugs is a complex phenomenon that manifests itself between drug and patient-specific variables that include, disease, genetics, age, sex and ethnicity (Ette and Williams, 2007). The Michaelis-Menten equation has had many biological applications from enzyme kinetics, membrane transport carrier to ligand-receptor binding and many more applications (Aksnes and Egge, 1991; Johnson and Goody, 2011; Portier et al., 1993). The body is assumed to have a finite volume where encountered particles can be handled. The Michaelis-Menten equation is used to model relative uptake. This is in order to mimic potential diffusion expected in the movement of the drug in the body as suggested by others (Yilmaz et al., 2012). There is no human data on absolute oral bioavailability of efavirenz to date (Cristofoletti et al., 2013). An important ratio the "relative uptake" (Total amount of drug reaching systemic circulation)/(cumulative uptake-volume at the point of full absorption) = A/V in modelling transportation is introduced. These results were extended and it was observed that the cumulative uptake volume could be modelled as a time dependent parameter.

A new way of modelling was introduced which enabled development of parameter estimates and this allowed better predictions of what possibly could occur within the body. Instead of using the time variable space only, there was the capturing of effects that are attributable to the covariate space as well. Furthermore, a proposition of an alternate way of interpretation of compartments and parameters is made.

MATERIALS AND METHODS

Patient data was obtained from Nyakutira et al. (2008) and only 61 patients were considered because they had the complete data for the following investigated independent variables, that is gender, weight and CYP2B6 G516T genotype. The patients were on TB treatment with a regimen containing rifampcin and also on stavudine and lamivudine as part of their HAART. Partial least squares regression (PLS) was used to generate a covariate function that was then projected into NONMEM for the estimation of middose concentration and other PK parameters. The following software packages were used to develop models in this work SIMCA, STATA, SPSS, NONMEM, and R. Non linear mixed effects modelling software brings data and models together, implementing an estimation method for finding parameters for the structural, statistical and covariate models that describe the data set (Mould and Upton, 2013). Clustering method(s) are used to identify subgroups that occupy different PK/PD response space. Clustering is a descriptive method that divides groups into a finite set of categories in order to capture the natural structure of data.

RESULTS

Primarily, estimations of mid-dose concentration in the sub-populations and the uptake-volume associated with the complete absorption of efavirenz were done. Sub-population in this work relates to a group of individuals in a population sample with the same characteristics that relates to the response variable and are projected to be in the same neighbourhood in the response space. The assumptions included the following:

time was considered initially constant, mid-dose plasma concentration(s) (x) were considered to be in the neighbourhood *(N)* of the point associated with complete absorption

$$(x_f)\{(x_f(t_a): t_a \geq t_{max})\ singleton, x(t) \in N(x_f) \subseteq (c_{min}, c_{max})\ for\ t \geq t_{max}\}$$

and were reflective of the total fraction absorbed in the systemic circulation, and the existence of a fixed finite carrying system (cumulative uptake-volume-enabling measurement of absorption time period) associated with the full dose of efavirenz. The assumption with respect to time was taken due to the fact that efavirenz has a long

Table 1. Predicted 12 h post plasma efavirenz concentration in relation to dose taken.

Covariate (φ)	Patient Description	n	Median Conc. (c_{md})	Predictions 600 mg		Prediction 400 mg		Prediction 200 mg	
				PLSR	NONMEM	PLSR	NONMEM	PLSR	NONMEM
0.05831	M,GG,W≥62	3	2.53	1.68	0.94	1.12	0.63	0.56	0.31
0.15339	M,GT,W≥62	5	3.27	2.53	2.30	1.69	1.53	0.84	0.77
0.23247	M,GG,W<62	5	3.52	3.24	3.28	2.16	2.19	1.08	1.09
0.23661	F,GG,W≥62	2	3.18	3.28	3.33	2.19	2.22	1.09	1.11
0.32754	M,GT,W<62	5	3.31	4.09	4.29	2.73	2.86	1.36	1.43
0.33169	F,GT,W≥62	9	3.2	4.13	4.33	2.75	2.89	1.38	1.44
0.41076	F,GG,W<62	3	3.64	4.84	5.05	3.22	3.37	1.61	1.68
0.50584	F,GT,W<62	13	4.9	5.69	5.78	3.79	3.85	1.9	1.93
0.58386	M,TT,W≥62	6	7.23	6.39	6.29	4.26	4.19	2.13	2.10
0.75802	M,TT,W<62	1	9.25	7.95	7.15	5.3	4.77	2.65	2.38
0.76216	F,TT,W≥62	4	8.17	7.98	7.17	5.32	4.78	2.66	2.39
0.93631	F,TT,W<62	5	9.14	9.54	7.72	6.36	5.15	3.18	2.57

half life (Almond et al., 2005; Yilmaz et al., 2012). This enabled the modelling of change in concentration post 12 h [in the 4 h-period sampled (12 to 16 h)] as being affected by the covariate structure only that excludes time. A relation that had been established as a link between genotype, gender and weight and the plasma efavirenz concentrations was used (Nemaura et al., 2012). Estimates for cumulative uptake-volume at the point of full absorption and estimated post 12 h concentrations were obtained. A one-compartment model (model 1a) was used:

$$\frac{dS_{PRE}}{d\varphi} = -g_d S_{PRE} \qquad (1.1)$$

$$\frac{dS_{FLOW}}{d\varphi} = g_d S_{PRE} - g_e S_{FLOW} \qquad (1.2)$$

Changes in concentration were considered to be affected by the covariate structure (φ-a variable that define the potential trend in drug levels almost surely in differing sub-populations). The covariate structure included weight, gender and genetic information of CYP2B6 G516T. Where S_{PRE} represented the pre-uptake compartment for the drug and S_{FLOW} represent uptake compartment where depositing and elimination took place. The parameter g_d was defined as a depositing relative constant which was 1 per covariate (φ) unit. The part eliminated was defined by g_e. The results in Nemaura et al. (2012) were extended in derivation of an algorithm proposed therein (Table 1). The number of clusters (*ń(CYP 2B6 G516T)* ń (S)*ń(W)=3*2*2=12, ń* is the number of categories) formulated was exhaustive. The investigated variables spanned the population. It was sufficient to use the previous boundary of 4 µg/ml to estimate doses because it separated the data in an almost 1:1 ratio, in this case it was 56:44 and furthermore the clusters spanned the population. Otherwise the median plasma concentration would have been used for separation in the development of a monotone function. The extensions of projected plasma concentrations for 200 and 400 mg were linear extrapolations (proportions) projected from the 600 mg dose.

A large variation on cumulative uptake-volume associated with full absorption (Typical Value of 35.6 L, ω_v = 0.8451) was observed. It was postulated that this may have been due to an insufficient wealth of information in the covariate structure that also includes time variable and possibilities of errors arising from accumulation of the drug at steady state.

In this case inclusion of information on possible covariates that affect efavirenz metabolism like CYP2B6 T983C, CYP2A6 and UGT 2B7 (Habtewold et al., 2011; Jiang et al., 2013; Ribaudo et al., 2011) could help and also other demographic information.

NONMEM (model 1(a)) projected one group to be in sub therapeutic concentrations, this group is of males who carry the CYP2B6 G516T GG genotype and of weight above 62 kg for individuals taking 600 mg. A dose of 800 mg was projected to have a typical value of 1.25 µg/ml.

The two methods that is PLS and NONMEM-PLS (Table 1) converged to similar points with NONMEM-SIMCA (PLS) (model 1(a)), giving a slightly improved estimation with regards to relationship between the covariate structure and concentrations predicted at mid-dose that excluded the time variable.

Estimation of bioavailability

A one-compartment model (model 1b) was employed with a transformation for φ to $\hat{\varphi}$ in order to estimate the eliminated fraction (presystemic) for every full dose of efavirenz (that is to find the existence of g_e such that $0 \leq g_e \leq 1$). There exist a $\hat{\varphi}$ for the found φ (equation 1.3) with the following properties:

$$\{\hat{\varphi} \geq 0 | \rho(\hat{\varphi}, c_{md}) = -r, \rho(\varphi, c_{md}) = r\}$$

and

$$\hat{\varphi} = m_{\varphi, c_{md}} \left(0.5 - \frac{1}{m_{\varphi, c_{md}}} (\varphi - 0.5) \right) \qquad (1.3)$$

Where r (r = 0.95 in the case considered), was the correlation between φ and c_{md}-median sub-population plasma concentration (Table 1) and $m_{\varphi, c_{md}}$ was the gradient of the line φ on c_{md} with $x(\varphi = 0) \in N(x_{min})$, x_{min} was the minimum efavirenz concentration in the population a potential possible asymptote. A fixed value of uptake-volume associated with complete absorption was approximated and a depositing relative constant with a fixed value of 1 to ensure full mass transfer was used. It was important for the run to converge to a global minimum (to ensure convergence in the covariate space). The resultant estimations gave rise to the following estimation for bioavailability ($1 - g_e$) based on cumulative uptake-volume of 35.56 L. A sufficient relationship between the observed plasma concentration *(x)* at steady state (12 to 16 h) and estimated fraction f reaching systemic circulation from the population sample was fitted (equation 1.4). There was no patient below 1 µg/ml in this population sample.

$$f = \frac{x^{1.121}}{x^{1.121} + 3.135^{1.121}}, R^2 = 0.98. \qquad (1.4)$$

The projected function f was easily noted to be an increasing function with respect to plasma concentrations at mid-dose interval, consequently showing that individuals with higher concentrations had correspondingly higher bioavailability. However, it was to be noted that the resultant estimates for bioavailability could have relatively large errors for those with higher concentrations as it was difficult to extrapolate the accumulation factor in concentration at this stage.

Inclusion of time and covariates in models

The time variable space was then included in modelling the mid-dose plasma concentrations at steady state. A one-compartment model was employed, defined by the following equations.

$$\frac{dS_{PRE}}{dt} = -k_d S_{PRE} \qquad (1.5)$$

$$\frac{dS_{FLOW}}{dt} = k_d S_{PRE} - k_e S_{FLOW} \qquad (1.6)$$

Where $k_e = \frac{ER_v}{V} = \frac{ER}{V}$, ER was the elimination rate (measured in $\frac{L}{h}$) at the point of full absorption, k_d depositing rate constant and V was the cumulative uptake volume associated with full absorption. Below is a set of results for the two models one with the estimated bioavailability and the other model which retained the current modeling framework of a central compartment and the input compartment (Table 2).

Model 2a (Figures 1 and 2): was based on the current compartmental modelling framework where there is a central compartment (S_{FLOW} with *A*-amount reaching systemic circulation) which represented plasma concentration and S_{PRE} represents the gut *(Dose-A)* and the other is defined as follows: S_{PRE} represents pre-uptake compartment of the drug in the systemic circulation and S_{FLOW} represents uptake compartment of depositing and elimination (in systemic circulation) (model 2b (Figures 3 and 4)). Model 2a carried the assumption that cumulative uptake-volume at the point of full absorption was equal to the volume of distribution. Considering Model 2b, only *A*-(Amount reaching systemic circulation) was used in the structural models.

Model 2b:

$$x_u(t) = \frac{A}{V(1 - k_e)} (e^{-k_e t} - e^{-t})$$

$x_u(t)$: (a solution of 1.1 and 1.2) approximated $x(t)$ the plasma concentrations in the neighbourhood of the end of absorption phase and post absorption phase. Furthermore, $x_u(t)$ approximated $x(t)$ at terminal points for large t and small $k_e = \frac{ER}{V}$. At the point where absorption ended the following condition hold

Table 2. Parameter estimations for two models with different values of bioavailability.

Parameter/Description	Value/equation	
	Model 2a (with bioavailability of 1)	**Model 2b (estimated bioavailability)**
OFV[#]	205	136
V(L)	35.56 FIX	35.56 FIX
ER_v (L/h)	3.09	1.374
k_a/h (k_d/h)	0.19776	(1 FIX)
ω_{ER}	0.605	0.239
ω_v	0.03	0.03
Observed mid dose concentration *x* vs. population prediction *y*	*y=0.1368x+4.1773, R^2 = 0.1702*	*y=2.6494+0.4056x, R^2 =0.7754*

[#] OFV= Objective Functional Value.

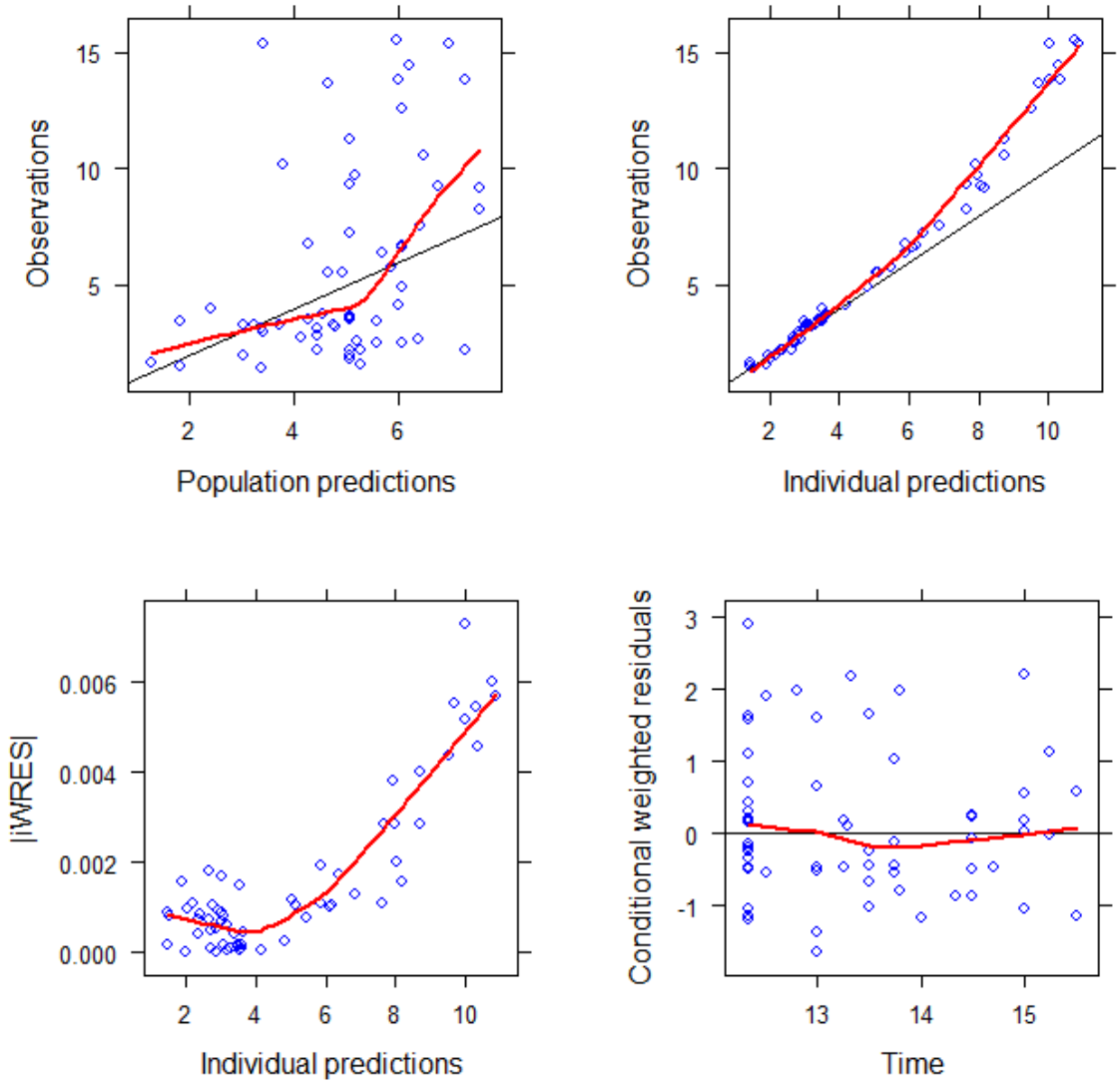

Figure 1. Goodness of fit plots for model 2a with bioavailability as 1.

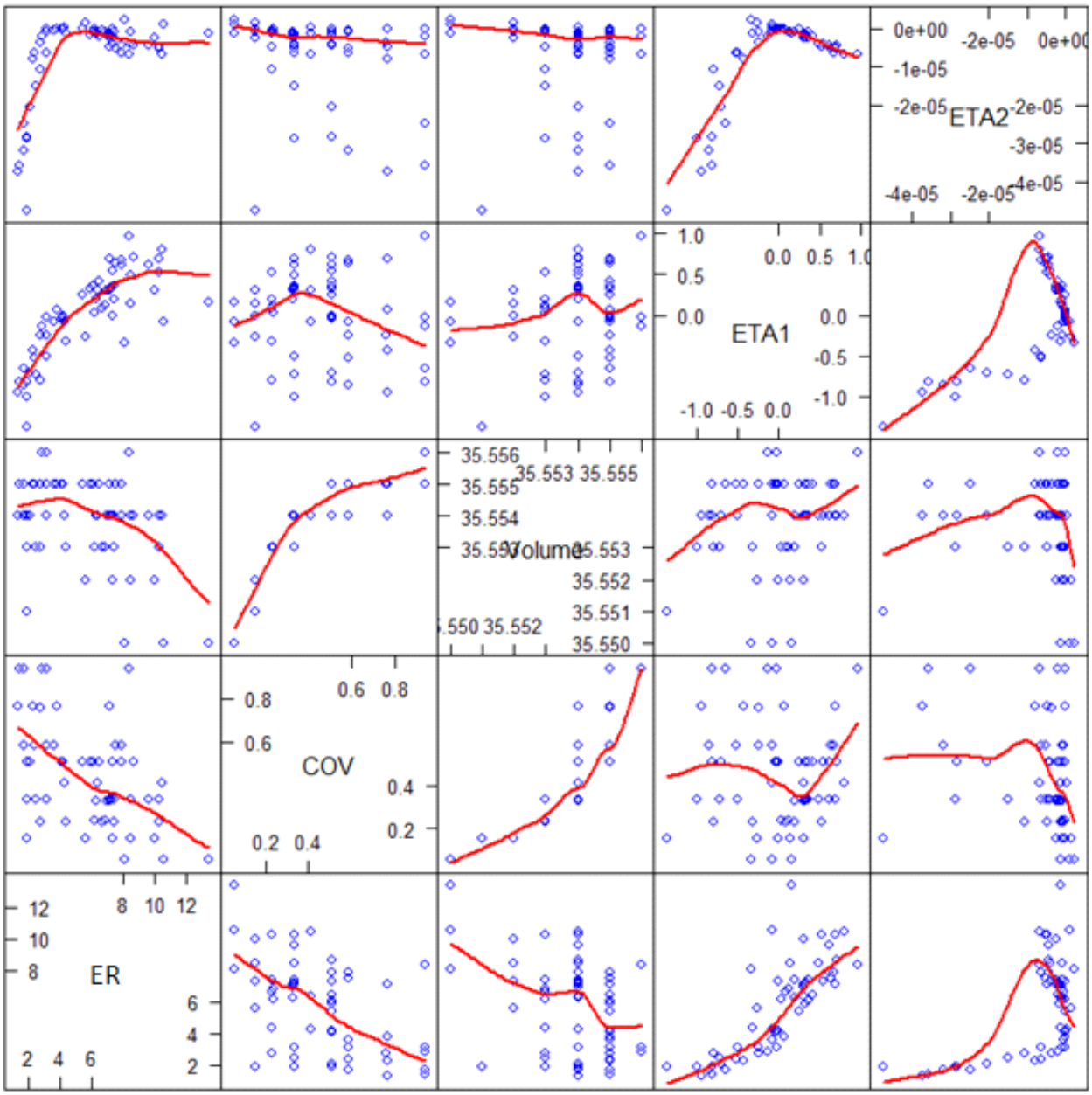

Figure 2. Scatter plot matrix showing how volume of distribution and elimination rate (clearance) and the covariate relation are related to each other model 2a.

$x_u(t_a) = x(t_a) = x_f$. A was the total amount that reached systemic circulation and V was the cumulative uptake volume associated with the complete absorption of A in the systemic circulation. The function $x_u(t)$ was used because of the two properties it exhibits. The definition and construction allowed the taking of the full fraction (total mass transfer of available drug) of the absorbed drug at any time t (A_t-the cumulative amount at time t) and per unit time. The ability to approximate the tail more favourably to the value $A/V * exp\ (-k_e t)$ since absorption was projected to be relatively low or close to zero after some time because of the decreasing amount of the drug in presystemic circulation, moreso for efavirenz with a long half life the terminal points of $x_u(t)$ then gravitates towards $A/V * exp\ (-k_e t)$.

Figures 1 to 4 show goodness of fit plots and scatter

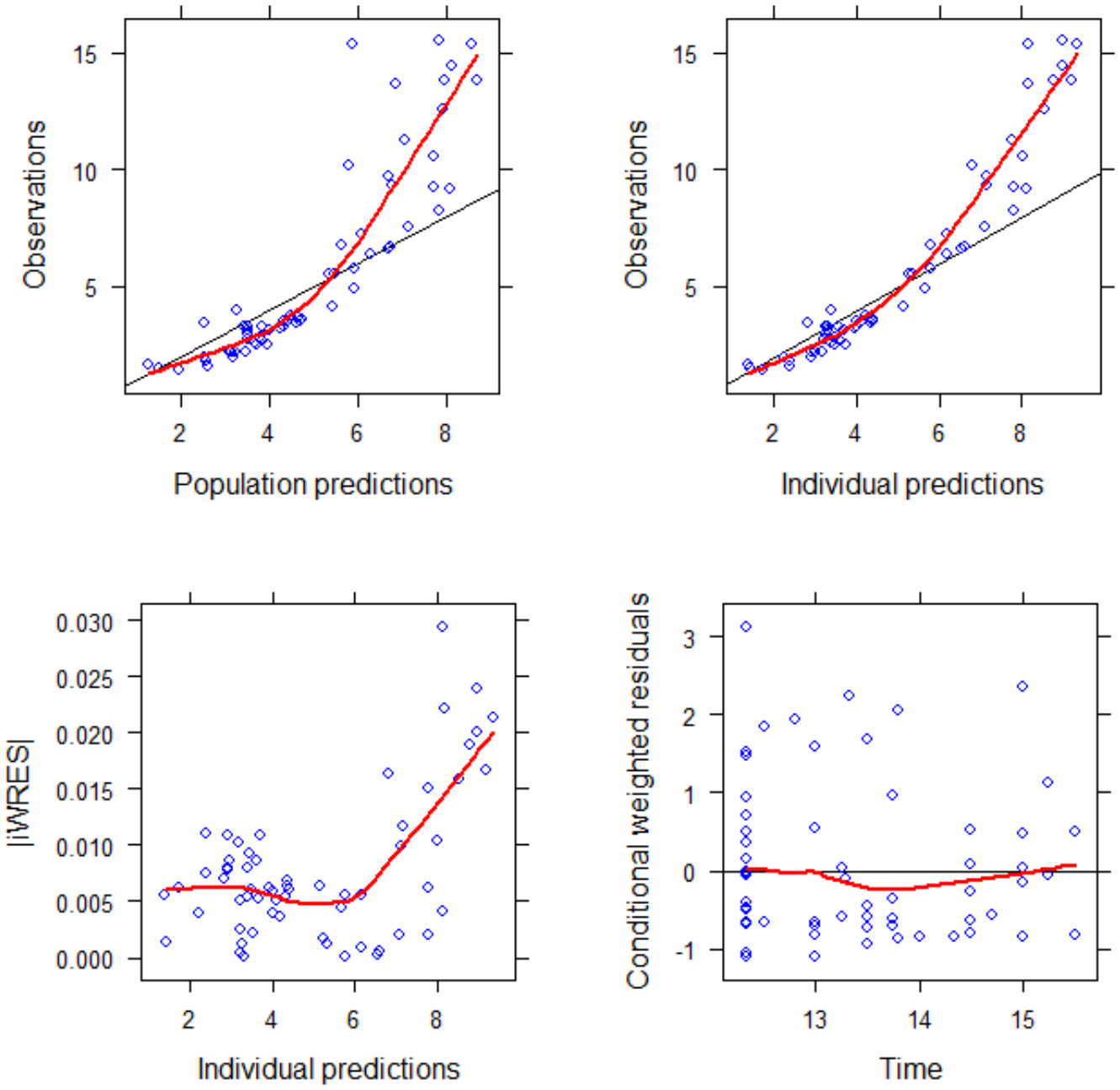

Figure 3. Goodness of fit plots for model 2b with the estimated varying bioavailability.

plots for the models 2a and b. The goodness of fit plots showed larger errors at higher concentrations. However, the models were formulated with the combined error model that takes into account both additional and proportional error. Model 2b was an improved model of 2a (a significant level of $p<0.01$ [$\Delta OFV=69>6.63$, *d f* (degrees of freedom) =*1*)].

The solid red line represents the median observed plasma concentration and the semi-transparent red field represents a simulation-based 95% confidence interval for the median (Figure 5). The observed 5 and 95% percentiles are represented with dashed red lines, and the 95% confidence intervals for the corresponding model predicted percentiles are shown as semi-transparent blue fields. Blue points represent the observed plasma concentrations. From the VPC, the model underestimated patients with high plasma efavirenz concentrations. The underestimation could be as a result of the data set not being corrected for accumulation, a consideration made in the next section

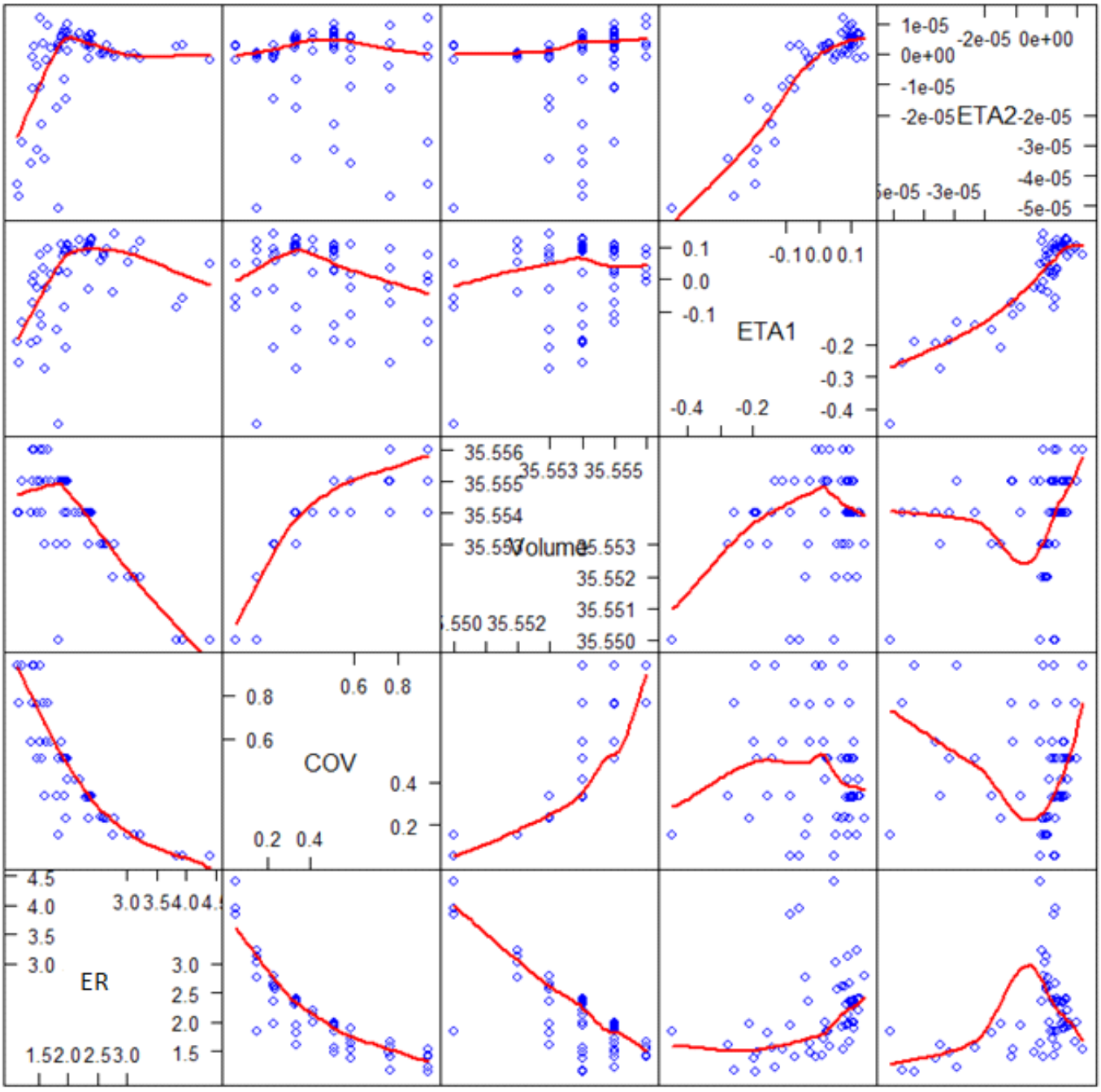

Figure 4. Scatter plot matrix showing how uptake-volume and elimination rate at the point of full absorption and covariate relation are related to each other model 2b.

(Toutain et al., 2004a) among other issues related to the drug efavirenz and its interaction with the body is made. Thus the patients with relatively higher concentrations with low elimination rates are expected to have higher accumulation thereby resulting in large errors. When the dosing interval is long comparative to the time required to eliminate the drug, accumulation is projected to be low. When the dosing interval is short in relation to the time needed to eliminate the drug, accumulation is high (this could be the case for individuals carrying the TT genotype). The projections of bioavailability, elimination rate constant and plasma concentrations are summarised including the elimination half life (Tables 3 and 4, Figures 6 and 7). These results are developed from model 2b.

The estimated amount of drug that reaches the targets (systemic circulation) for poor metabolisers is greater than that of fast metabolisers. A multiple linear regression model was developed for the three variables terminal

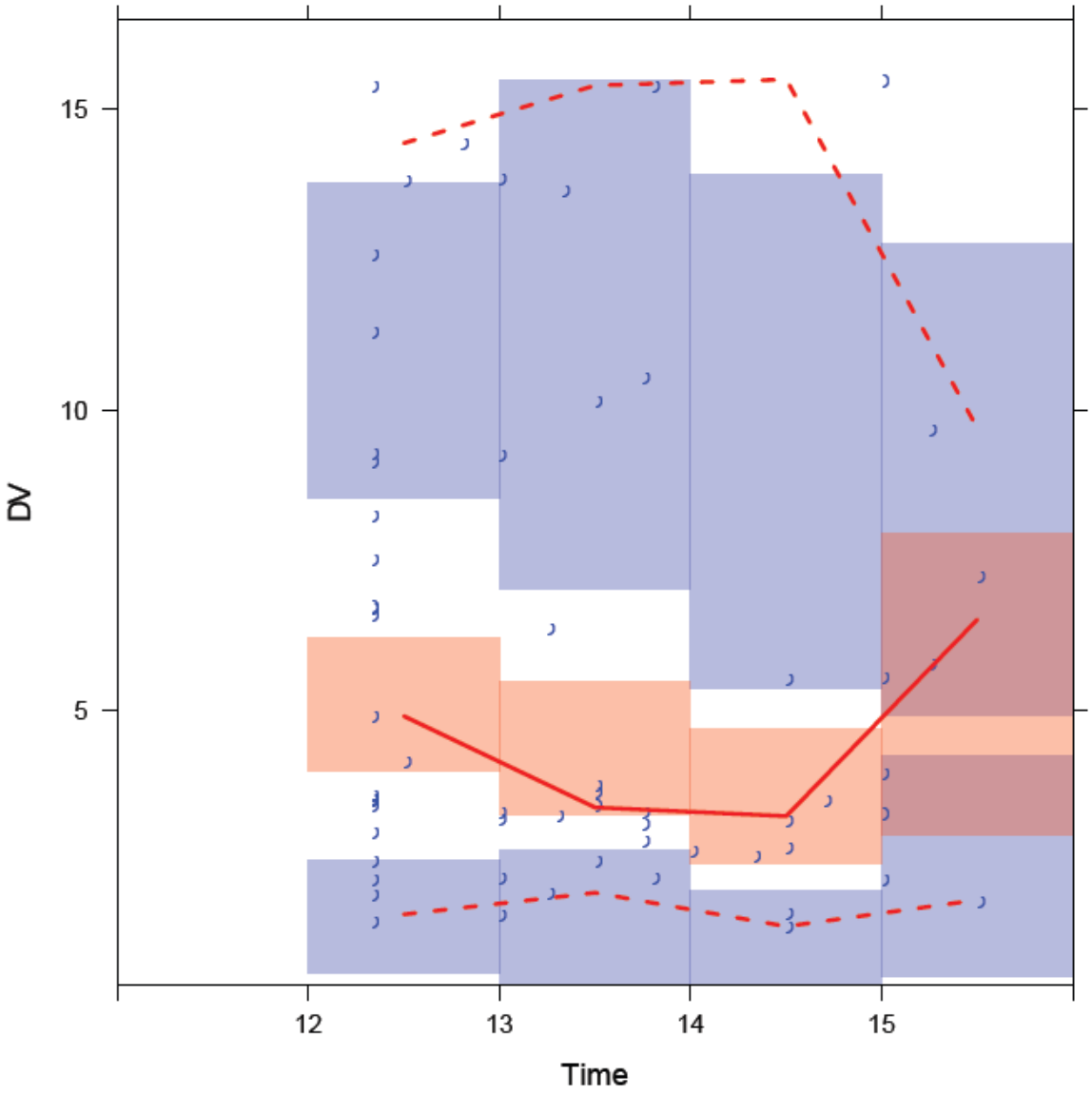

Figure 5. The value predictive check (VPC) for the terminal plasma concentration for model 2(b).

Table 3. Summary statistics showing median and interquartile ranges of plasma concentration at steady state, bioavailability, and elimination rate constant.

Variable	Median (IQR)
Plasma Conc. (µg/ml)	3.6 (2.72,8.25)
f.	0.65 (0.55,0.85)
k_e(/h)	0.056 (0.047,0.067)

plasma concentration *(x),* elimination rate constant *(k_e)* and oral bioavailability *(f); ln x = 3.3995f - 8.0614k_e* (Table 5). The rationale being that the concentrations observed are functions of both bioavailability and elimination related variables.

Factoring in correction of accumulation of the drug at steady state in modeling mid-dose concentrations-predicted results after only a single dose is taken

The results were extended by considering a model which corrected for accumulation brought about by continual taking in of the drug efavirenz at steady state. An accumulation factor of $a_{f,ss} = \frac{1}{(1-e^{-k_e\tau})}$ (where $\tau = 24hrs$ is a dosing interval) was used to correct for the mid-dose plasma concentrations at steady state. The elimination rate constant was estimated from model 2b, which had steady state conditions in order to form model 2bi (Table 6, Figures 8 and 9) which did negate accumulation. The solid red line represents the median

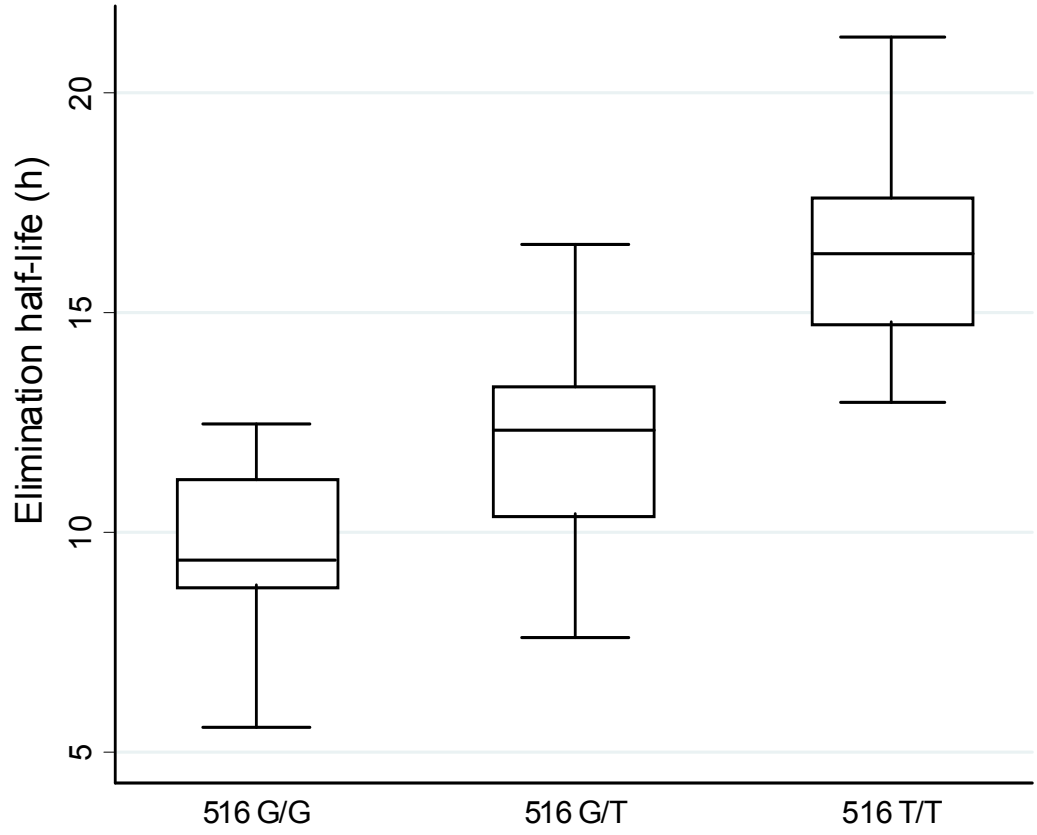

Figure 6. Estimated elimination half-life (h) for GG, GT, and TT genotypes of CYP2B6, the median (IQR; Interquartile range) times are as follows 9.4 (8.8, 11.2), 12.3 (10.4, 13.3) and 16.3 (14.8, 17.6), respectively.

Table 4. Correlations between *f, k_e*, and mid-dose efavirenz plasma concentration.

Variable	Plasma Conc.	f	k_e
Plasma Conc.	1	-	-
f.	0.92	1	
k_e	-0.64	-0.57	1

Table 5. Coefficients of the multiple linear regression model of 61 patients at steady state for plasma concentration (x) at t= (12 to 16 h), elimination rate constant (k_e) and oral bioavailability (f) (ln x=β_1f+$\beta_2 k_e$ (Multiple R-square = 0.9975)).

Coefficients	Estimate	Standard Error	p-value
β_1	3.3995	0.0353	p<0.0001
β_2	-8.0614	0.3459	p<0.0001

observed plasma concentration and the semi-transparent red field represents a simulation-based 95% confidence interval for the median (Figure 10). The observed 5% and 95% percentiles are represented with *dashed red lines*, and the 95% confidence intervals for the corresponding model predicted percentiles are shown as semi-transparent blue fields. Blue points represent the observed plasma concentrations (corrected for accumulation). The most notable improvement was noted in the difference in objective functional value (OFV). Model 2bi was found to be an improvement of model 2b, the difference is highly statistically significant with an OFV difference of 75. The median and interquartile range (IQR) of the elimination rate constant of model 2bi was 0.0874(0.0758, 0.0933). The plasma concentration was shown to be positively correlated to bioavailability and negatively correlated with the elimination rate constant (Table 7). A multivariate model was developed for the relationship between *f, k_e,* and mid-dose interval efavirenz plasma concentration at steady state; $\ln x = 3.609f - 7.1794k_e, R^2 = 0.9975$, established from model 2bi.

Extension

Transportation in the human body for an orally administered drug, volume of distribution and AUC

The results and extensions used in this section are mainly based on simulations from model 2b, because the concentrations were at steady state. At any given time t,

Table 6. Parameter estimation for model extension of model 2(b) that accounted/corrected for the accumulation at steady state.

Parameter	Value/equation
OFV[#]	61.34
V(L)	35.56 FIX
ER_v (L/h)	2.578
k_d/h	1 FIX
ω_{ER}	0.1748
ω_v	0.003
Observed mid dose concentration (corrected for accumulation) x_{acc} vs. population prediction y	$y=0.455x_{acc}+1.759$, $R^2 = 0.803$

Estimated bioavailability [model 2(bi)]. [#] OFV= Objective Functional Value.

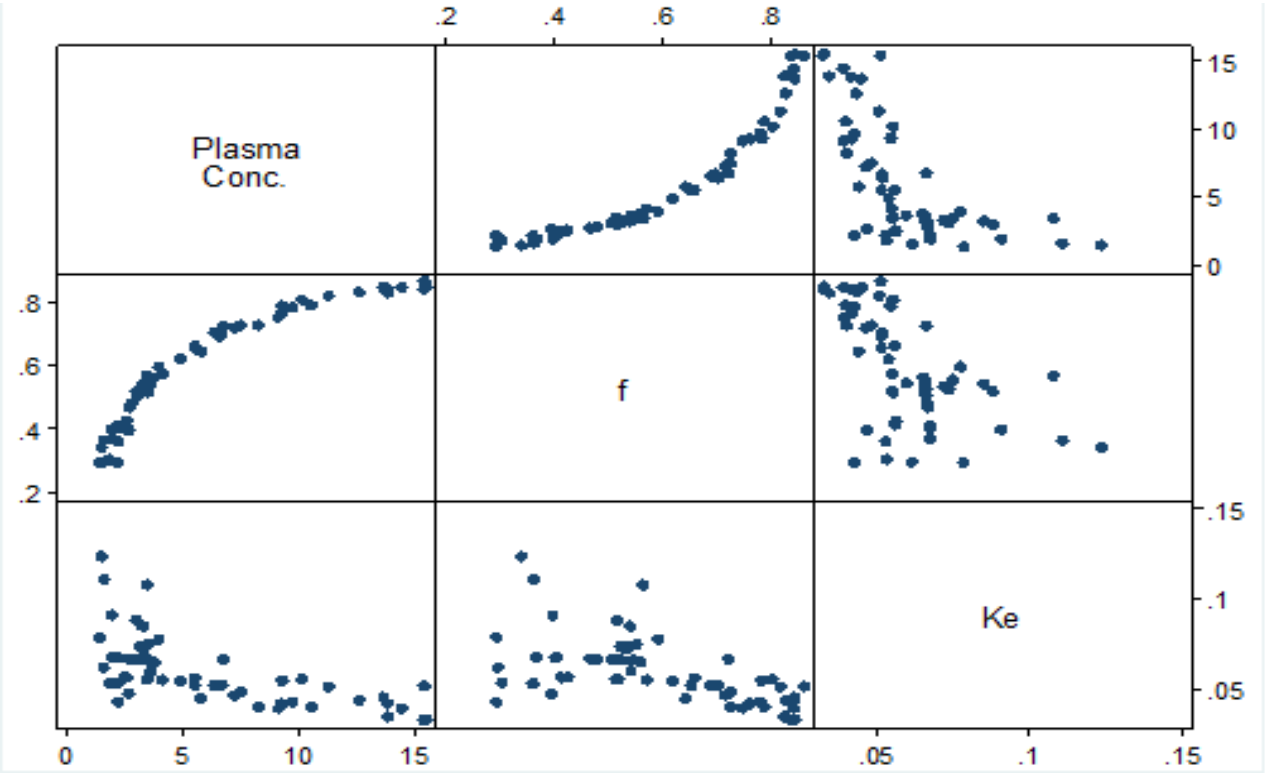

Figure 7. Scatter plot matrix of elimination rate constant k_e, 12 to 16 h post dose plasma concentration and bioavailability *f*.

$\frac{A}{V} = \frac{A_t}{V_t}$ and $\frac{ER}{V} = \frac{ER V_t}{V_t} = k_e$ are assumed to be constants (equation 1.7) (A_t was the accumulating drug in the systemic circulation and V_t was the uptake volume space covered by A_t, ER was the elimination rate at the point of full absorption, A was the total amount reaching the systemic circulation and V was the cumulative uptake volume associated with full absorption of A). The cumulative uptake-volume followed a saturation curve. The cumulative uptake volume moved from $V = 0L$, at $t = 0$ to a $V = V(A) \leq V(t \to \infty)$, where $V(A)$ was the cumulative uptake-volume associated with the full absorption of A. The cumulative uptake-volume V_t was observed to be a time dependent variable and the movement of A across V was facilitated by transportation mechanisms within the body (facilitated diffusion). The relation-ship between the drug uptake relative to volume-$\frac{A}{V}$ (dependent variable) and 'concentration' $x_u(t)$ (independent) was assumed to follow Michaelis-Menten

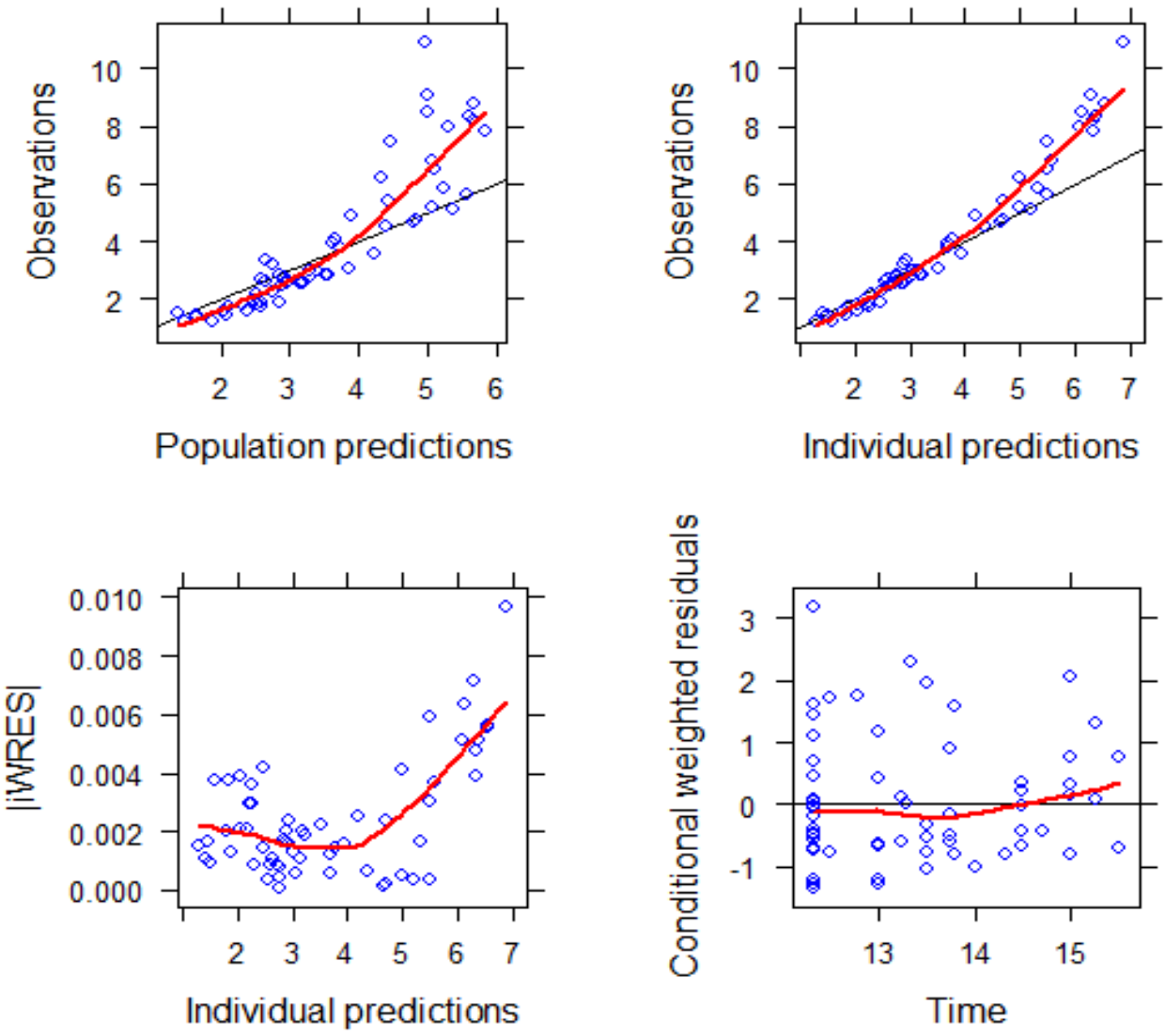

Figure 8. Goodness of fit plots for model 2bi with the estimated varying bioavailability and concentrations corrected for accumulation.

equation. Michaelis-Menten equation was used because of the saturation mechanism in relation to the cumulative uptake-volume associated with the uptake of the drug and the movement of A was projected to be facilitated (diffusion) by transportation mechanisms within the body. This was the main motivation for the use of the Michaelis-Menten equation below (equation 1.8). Primarily, the pharmacokinetic curve of an orally administered drug follows a biexponential curve with respect to time. A proposition was made such that for an oral dose that reached the systemic circulation, there exist a relationship for the uptake of A, defined by:

$$x_u(t) = \frac{A}{V(1-k_e)}(e^{-k_e t} - e^{-t}) \qquad (1.7)$$

for k_e small (small k_e improves convergence of $x_u(t)$ to $x(t)$-plasma concentration at terminal time points). The depositing rate constant was fixed to 1. The availability of occupation space (the uptake volume), elimination and transportation mechanism strongly influenced the availability of A in the systemic circulation. The relation between A/V and k_e at steady state is shown in Figure 11.

The Michaelis–Menten equation was used to describe the facilitated transport (a saturable process):

$$\frac{A}{V}=\frac{\left(\frac{Dose}{V}\right)_{max}x_u(t)}{k+x_u(t)}=\frac{A_t}{V_t}=\frac{\left(\frac{Dose}{V_t}\right)_{max}x_u(t)}{k+x_u(t)}=\frac{vx_u(t)}{k+x_u(t)},\text{where } V_t \leq \mathrm{V},\text{and } A_t \leq \mathrm{A} \quad (1.8)$$

The ratio $\frac{\mathrm{A}}{\mathrm{V}}$ is defined as the relative uptake and $\left(\frac{\mathrm{Dose}}{\mathrm{V}}\right)_{max}$ is the possible maximum relative uptake. This implies that for each t there exists a unique value of v. From v one could therefore obtain $\mathrm{V_t}$. It is important to stress that if the concentrations $x(t)$ are at steady state there is need to correct for accumulation by a factor of $\frac{1}{(1-\mathrm{e}^{-\mathrm{k_e}\tau})}$ where τ is a dosing interval. An asymmetrical sigmoid curve was then fitted for uptake volume against time, as this was sufficient for the data. In this case, two models were fit. The first model was for the whole sample of 61 patients' (model 3a) (where a naive assumption was made of equal transportation rates in all subjects) and the other one was where a relatively fast transportation at steady state was projected for one patient in the sample (model 3b) (an example of modelling one individual which could be extended to the whole group to obtain better estimated population parameters).

In the construction of model 3a, the facilitation here was assumed to be at the same rate in the group. The ratio $\frac{\mathrm{A}}{\mathrm{V}}$ being constant also implied that A and V may vary with respect to $time$ but their ratio did not. In other words A_t and uptake-volume were allowed to follow the same trajectory in terms of spread when A_t reached 100% (A) so did V_t as it assumed the value of cumulative uptake-volume associated with full absorption A. This was done primarily to capture the movement of A. The models estimated that generally in this population in 24 h, 90% of A (A is varying across individuals) will generally have reached systemic circulation (Table 8) at steady state. In this population the drug was projected to be fully absorbed after approximately 31 h (Figure 12 and Table 8). The accumulating percentage $A_{average}$ against $time$ was modelled. An asymmetrical sigmoid curve was found to be the best fit. This relationship could similarly have been observed for the cumulative uptake-volume.

A fit of a 5 parameter logistic regression (asymmetrical sigmoid curve (Figure 12)) was made and the following equation was obtained:

$$A_{average}=256.1598-\frac{255.9614}{\left(1+\left(\frac{t}{7.5247}\right)^{1.3786}\right)^{0.2365}},\qquad R^2=0.99999 \quad (1.9)$$

Points on the same line passing through the point $\left(0,\frac{Dose}{V}\right)$ share the same rate of percentage increase of drug absorbed relative to the full amount at any given time (that is the rate of uptake volume in m and w follow similar trends) (Figure 13). In this case the availability of A is directly linked/proportional to elimination rate that is:

$$A(=\mu ER_A+Dose)=\gamma ER_V+Dose \quad (1.10)$$

Dividing by $V\neq 0$ produces the linear relationships l_1, l_2 and l_3 (Figure 13). It can also be noted that:

$$AUC^{x_u(t)}{}_{\mathrm{m}} > AUC^{x_u(t)}{}_{\mathrm{n}} > AUC^{x_u(t)}{}_{\mathrm{u}} > AUC^{x_u(t)}{}_{\mathrm{v}} > AUC^{x_u(t)}{}_{\mathrm{w}}.$$

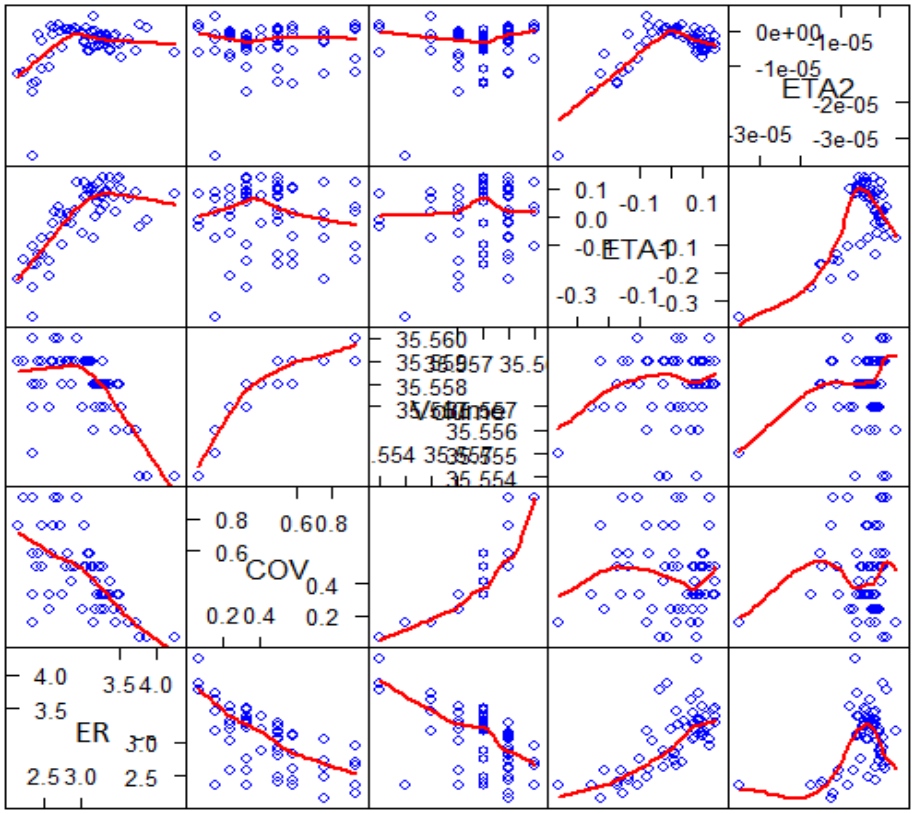

Figure 9. Scatter plot matrix showing how cumulative uptake-volume and elimination rate at the point of full absorption and covariate relation are related to each other for model 2b(i) with concentrations corrected for accumulation.

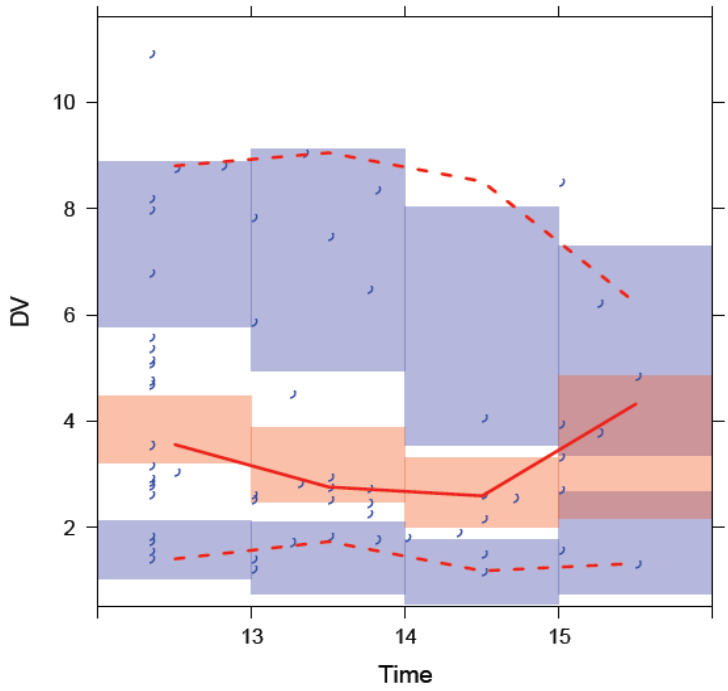

Figure 10. The value predictive check (VPC) for the terminal plasma concentration (corrected for accumulation) (500 samples were generated-bootstrapping method for the VPC).

Table 7. Correlations between *f*, k_e, and mid-dose interval efavirenz plasma concentration at steady state.

Variable	Plasma Conc.	f.	k_e
Plasma Conc.	1	-	-
f.	0.92	1	
k_e	-0.88	-0.83	1

$lnx = 3.609f - 7.1794k_e, R^2 = 0.9975$, established from model 2bi.

the individual P from eqn 1.7 using terminal points between C_{max} and C_{min} for the drug with the long half life.
2. Formulate the linear relationship such that the point $\left(k_e = 0, \frac{Dose}{V_P}\right)$ and $\left(k_{ep}, \frac{A}{V_P}\right)$ are on the line.
3. A range of points on the generated line are selected in the first quadrant (that is simulate individuals who have (share) the same transportation rates as P) (Table 9).
4. Equations 1.7 and 1.8 were then used to obtain the following results (Table 10).

$$A_{average} = 115.6782 - \frac{115.6568}{\left(1+\left(\frac{t}{13.1796}\right)^{1.1267}\right)^{8.8857}}, \qquad R^2 = 0.999996 \qquad (1.11)$$

Points lying on $l\left\{l: \frac{A}{V} = \gamma k_e + \frac{Dose}{V} \overset{\text{iff}}{\Leftrightarrow} A = \gamma ER_V + Dose\right\}$ with the least gradient (γ) have the fastest transportation in the sampled population. The elimination rate of A for the drug that reaches systemic circulation follows from the relationship $k_e V_t = ER_{V_t} \leq ER_V$. This follows a similar relationship to that of cumulative uptake volume and $A_{average}$ with respect to time in an individual. For a monophasic PK curve, $\frac{A(mg)}{V(L)} = A_t(mg)/V_t(L) = c(mg/L)$

$$A_t = cV_t \qquad (1.12)$$

$$\frac{Amount\ cleared\ per\ unit\ time}{Total\ Amount\ at\ time\ t} = \frac{ER_{A_t}(mg/hr)}{A_t(mg)} = \frac{ER_{A_t}(mg/hr)}{cV_t(mg)} = \frac{\frac{ER_{A_t}(mg/hr)}{c(mg/L)}}{V_t(L)} = \frac{ER_{V_t}(L/hr)}{V_t(L)} = k_e. \qquad (1.13)$$

From equation 1.13 one notes that:

$$ER_{A_t} = k_e A_t \qquad (1.14).$$

It is noted that from Equations 1.13 and 1.14, and by definition, the elimination rate constant can also be used to define the ratio of the amount of drug (disregarding volume) cleared per unit time to total amount in the body at a particular time. The elimination rate is primarily dependent on the total amount in the system. Correspondingly, A_t accumulates with V_t (up to the case when $A_t = A$ and $V_t = V$). The uptake volume V_t can also be used as a dummy for A_t (Equation 1.13).

The parameter ER_{A_t} relates to the elimination of the actual amount in the systemic circulation and ER_{V_t} relates to elimination associated with the cumulative uptake volume occupied by A_t. An estimation of the amount of drug cleared (Table 11, Figures 14 and 15) associated with the individual on quicker transportation in this sample population was done.

$$\mathrm{D_t} = \frac{\mathrm{A_t}}{\mathrm{A}}\mathrm{Dose} = \frac{\mathrm{V_t}}{\mathrm{V}}\mathrm{Dose} \qquad (1.15),$$

$$\mathrm{A_t} = \frac{\mathrm{V_t}}{\mathrm{V}}\mathrm{A} \qquad (1.16).$$

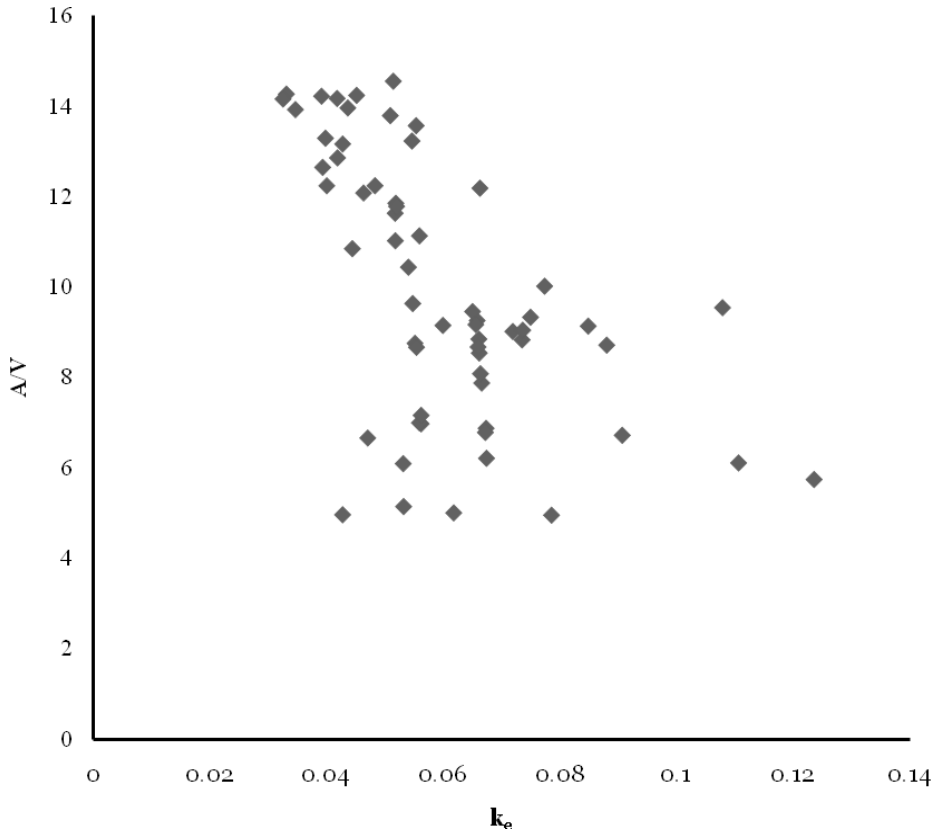

Figure 11. Graph showing evidence that of a negative correlation between $\frac{A}{V}$ and k_e for the 61 patients on efavirenz.

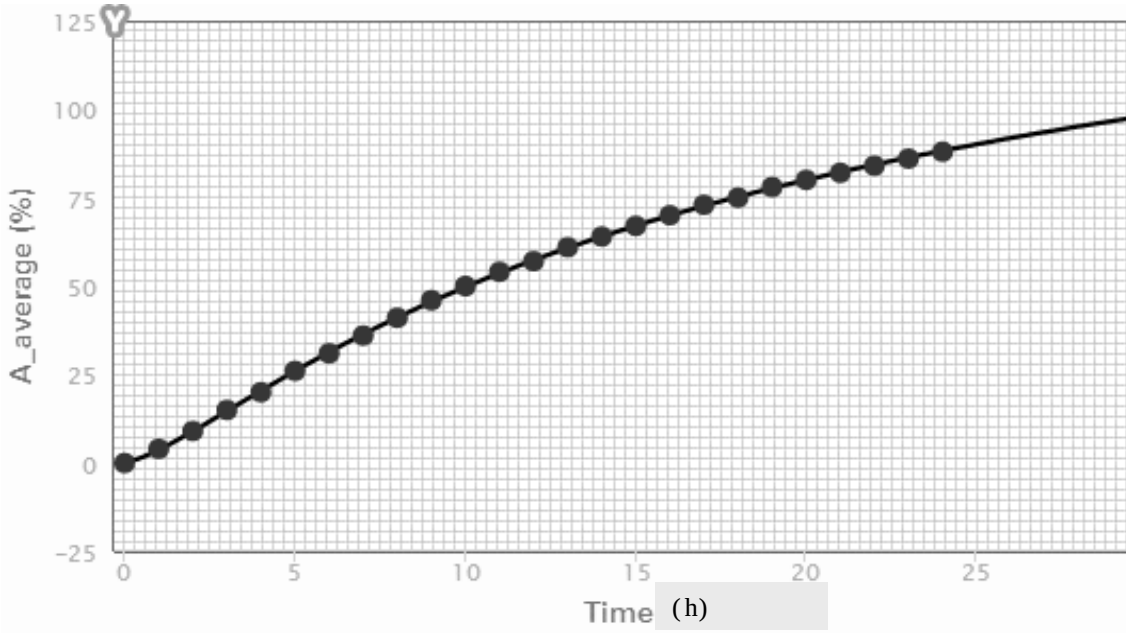

Figure 12. The five parameter logistic regression equation showing estimated average absorption time into the systemic circulation for the whole sample.

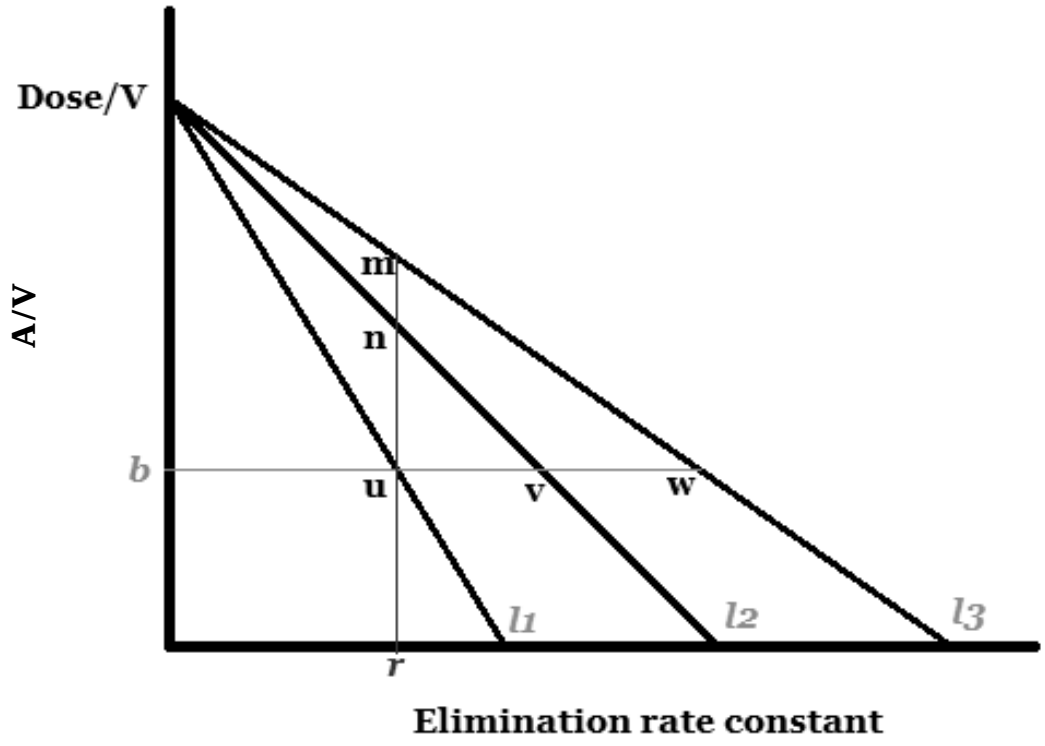

Figure 13. Illustration of relationships of the ratio $\frac{A}{V}$ and k_e between different individuals in a population.

A is full amount reaching systemic circulation and V is the corresponding cumulative uptake-volume associated with A's full absorption. The elimination rate constant is where one obtains the amount being eliminated from the systemic circulation please note $j = t$

$$A_1 k_e = Q_1$$
$$(A_2 - Q_1)k_e = Q_2$$
$$(A_j - Q_{j-1})k_e = Q_j$$

For patient P, points after absorption are well projected (Figure 16). Absorption was projected to end at the point reaching systemic circulation at time t) can be approximated by an asymmetrical sigmoid function. The estimated AUC's relation with mid-dose plasma I (x_f) in reference to patient P. The region in blue represents potential points where the concentration curve may have been laid (these may potentially be due to the volume occupied). All curves have to pass through the point I and point of origin (The assumption made was that there was no delayed absorption). The curve x represents the plasma concentration obtained by assuming maximum potential spread in the possible volume space (39.68 L) during the whole period. The patient's absorption rate at time $t,$ it is found by $AR(t) = \frac{dA_t}{dt}$ where A_t (cumulative amount concentration at steady state projected using the volume of distribution (V_d) of 39.68 L per individual in this population was given by:

$$AUC = f.Dose/CL = 16.35x, r = 0.9767\ (AUC_{SS} = AUC.a_{f,ss} = 24.79x, r = 0.9763)$$

The results were generated from models 2b and 2b (i), where $CL = k_e * V_d$. The patients carrying the *CYP2B6 G516T TT* genotype were projected to have higher exposure levels (Table 12).

DISCUSSION

A proposition is made that a multifactorial approach of using 516G > T together with routine clinical measurements of weight and gender status, in decisions

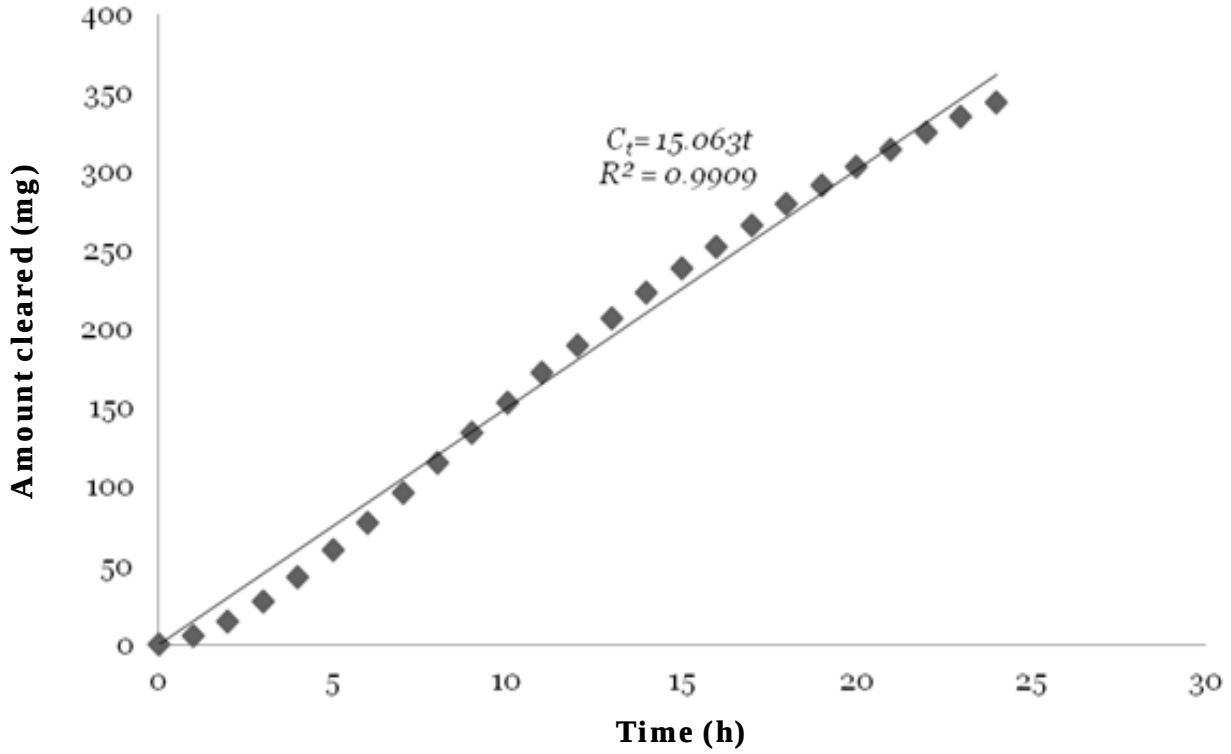

Figure 14. Estimated amount of drug cleared in systemic circulation in 24 h for patient P. The amount cleared was shown to be relatively constant (15 mg/h).

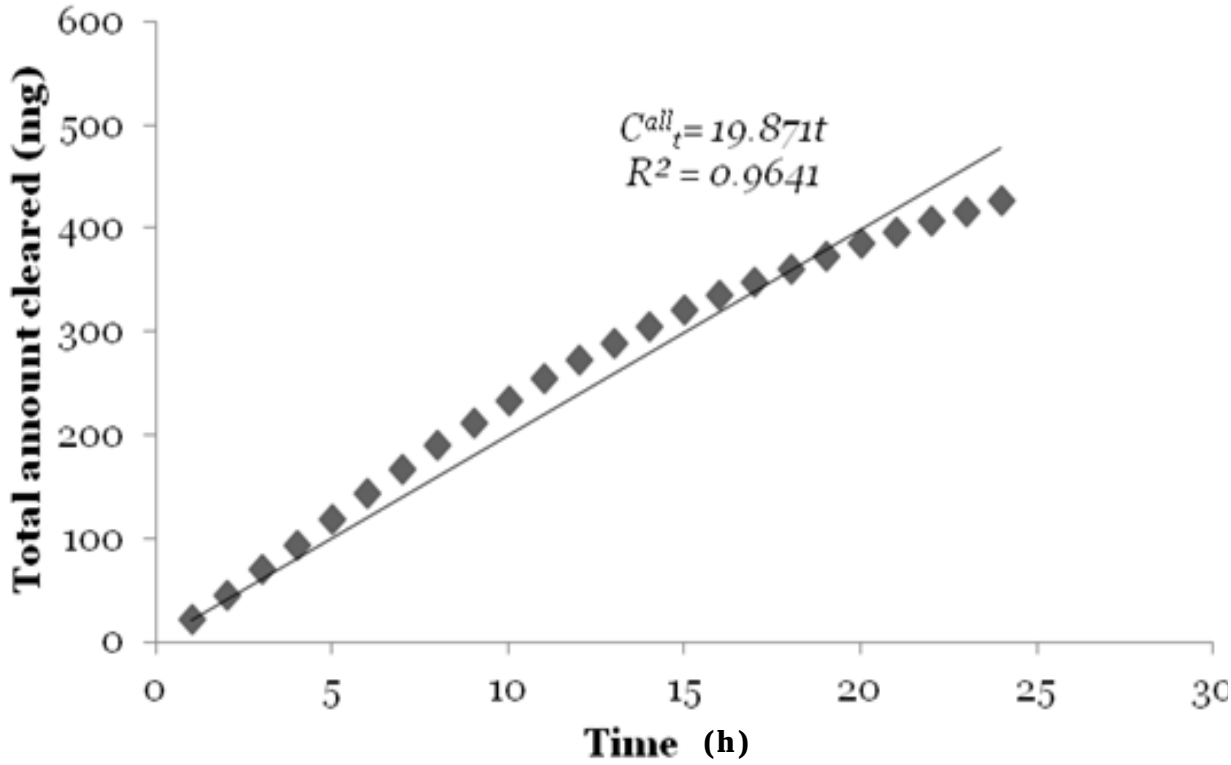

Figure 15. Estimated total amount of drug cleared in 24 h for patient P. The amount cleared was shown to be almost constant about 20 mg/h.

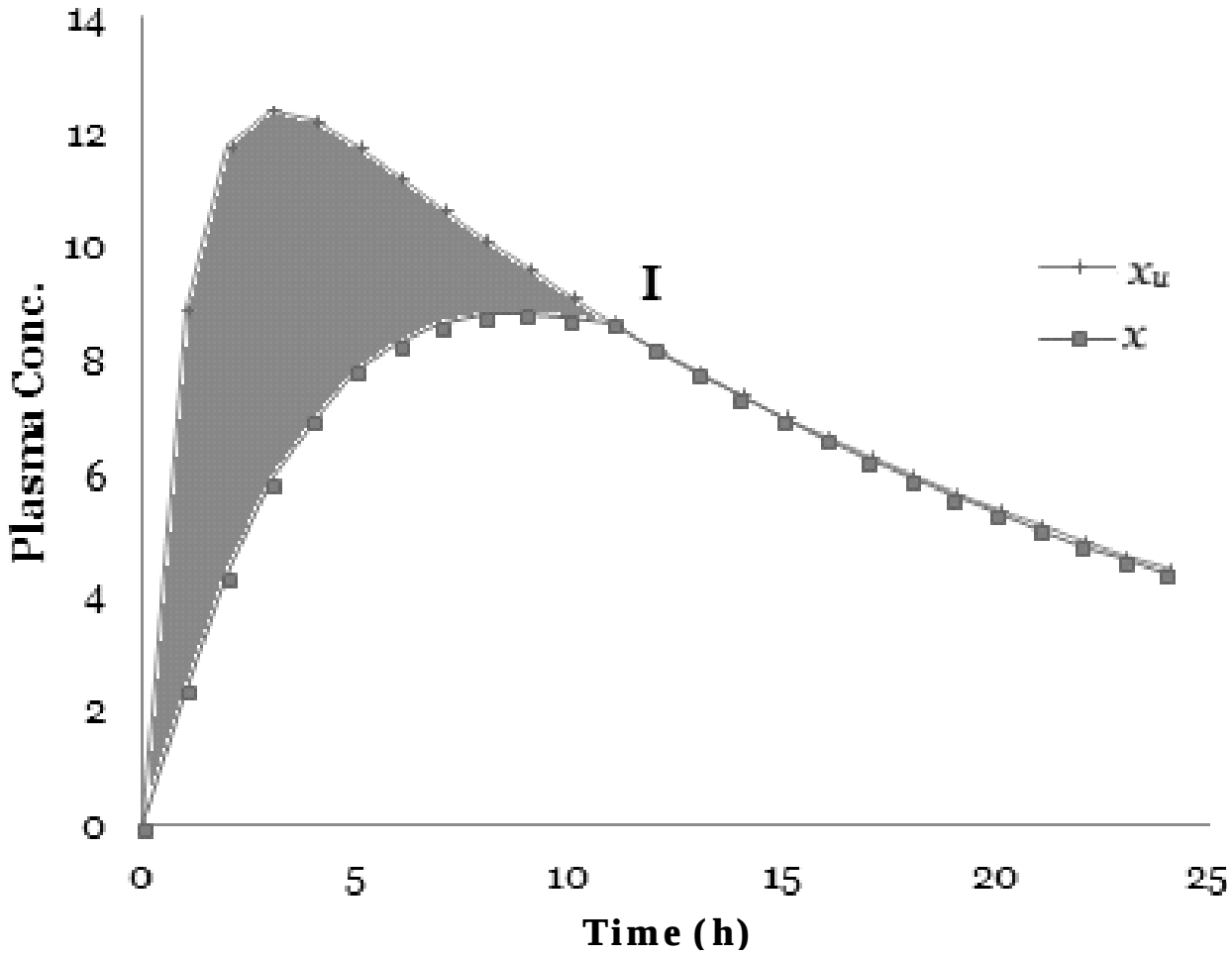

Figure 16. Projected plasma concentration- time curve for patient P.

on which patients are at risk of high efavirenz exposure (Table 1) and possibly CNS adverse drug reactions (Mukonzo et al., 2014). These patients with high efavirenz exposure may require dose reduction enabling less discontinuation of the drug efavirenz (Van Luin et al., 2009). The richer covariate information enables better estimates. Furthermore, more information on the covariate structure enables better correlations to be established between the covariates and the plasma concentration (Table 1). It is desirable to have full PK profiles (rich sampling) as these will guarantee monophasic profiles (one period). In addition, more robust estimates can be developed from the AUC generated from full profiles.

These results also point us towards an assumption that efavirenz is not a drug that hides in tissues due to the value of volume of distribution found but is a drug that is expected to distribute well within the body fluid volume system (Toutain et al., 2004b). This was supported by the fact that efavirenz is highly bound to plasma proteins (Cristofoletti et al., 2013; Rekić et al., 2011; Smith et al., 2001). However a different inference could be postulated from what others have found with regards to the volume of distribution (150 to 500 L) (Cristofoletti et al., 2013; Nyakutira et al., 2008; Ribaudo et al., 2006; Sánchez et al., 2011; Siccardi et al., 2012; Yilmaz et al., 2012), which could also be linked to the high lipophilicity of efavirenz (Cristofoletti et al., 2013).

The modelling not only improved estimates (Tables 2 and 6), but also the results showed how one can incurporate time and other variables that affect changes in concentration of efavirenz. As far as can be ascertained, these results in this work are the first that tried to estimate oral bioavailability based on an estimated value of a newly introduced cumulative uptake-volume associated with full absorption (and consider absorption as a cumulative process based on this cumulative uptake-volume). An asymmetric sigmoid relation was proposed for the relationship between efavirenz mid-dose concentration and bioavailability (equation 1.4). Other researchers have postulated on the potential impact which could be attributed to bioavailability on the esti-mation of efavirenz PK parameters (Csajka et al., 2003; Cabrera et al., 2009).

The current models in PK modelling define absorption as a continuous process that is not clearly defined as a

Table 8. Results showing average percentage of absorbed efavirenz in the systemic circulation in this population.

Time (t)	All patients (Model 3(a))				
	k	$(Dose/V)_{max}$	R_{square}	V_t	Average percentage absorbed relative to A $(A_{average})$
0	-	-	-	0	0
1	241.794	406.1381	0.9995	1.4773	4
2	139.172	184.1495	0.9974	3.2582	9
3	85.5356	114.8444	0.9935	5.2245	15
4	59.4248	82.7927	0.9877	7.2470	20
5	42.8447	64.9518	0.9803	9.2376	26
6	32.3415	53.8189	0.9716	11.1485	31
7	25.2901	46.3205	0.9618	12.9532	36
8	20.3153	40.9674	0.9512	14.6458	41
9	16.6609	36.9707	0.9399	16.2291	46
10	13.8876	33.8794	0.9282	17.7099	50
11	11.7264	31.4196	0.9161	19.0964	54
12	10.0056	29.4163	0.9037	20.3969	57
13	8.611	27.7530	0.891	21.6193	61
14	7.4637	26.3493	0.8781	22.771	64
15	6.5158	25.1641	0.8651	23.8435	67
16	5.714	24.13	0.8519	24.8653	70
17	5.0336	23.2268	0.8386	25.8322	73
18	4.4515	22.4306	0.8253	26.7492	75
19	3.9503	21.7232	0.8119	27.6202	78
20	3.516	21.09	0.7984	28.4495	80
21	3.1377	20.5195	0.7849	29.2405	82
22	2.8098	20.0126	0.7715	29.9811	84
23	2.5196	19.5444	0.7580	30.6993	86
24	2.2636	19.1163	0.7445	31.3869	88
31	1.1143	16.907	0.651	35.4883	100

Table 9. Simulated individuals carrying similar transportation rates as patient P.

k_e	$\frac{A}{V}$
0	16.85393
*(P=)*0.051531	14.55997
0.26703	4.966767
0.179937	8.843835
0.168722	9.343091
0.104649	12.19535
0.073601	13.57749
0.175802	9.027896
0.175151	9.056887
0.201422	7.887409
0.186481	8.552503
0.32379	2.44
0.356138	1
0.378602	0

Table 10. Results showing average percentage of absorbed efavirenz in the systemic circulation for the individual exhibiting fastest transportation in this population.

Time (t)	Patient (model 3(b))				
	k	$\frac{Dose}{V}_{max}$	R_{square}	V_t	Estimated Percentage absorbed relative to A $(A_{average})$
0	-	-	-	0	0
1	46.0809	89.6937	0.999998	6.6894	19
2	26.0169	46.7984	0.999966	12.8210	36
3	15.8841	33.3180	0.999795	18.0083	51
4	10.3502	27.0212	0.999314	22.2048	62
5	7.0993	23.4919	0.9984	25.5407	72
6	5.0644	21.2833	0.9968	28.1911	79
7	3.7221	19.7937	0.9947	30.3127	85
8	2.7976	18.7302	0.9920	32.0338	90
9	2.1392	17.9384	0.9888	33.4478	94
10	1.6577	17.3291	0.9851	34.6238	97
11	1.2981	16.8475	0.9811	35.6136	100

terminating process at some point in time. Furthermore, other researchers have noted the need to characterise drug absorption as most models lack physiological rationale (Ette and Williams, 2007). The work also introduced how one can incorporate two spaces that help us estimate changes in drug concentration in the body, that is the covariate space and the time space. A marked improvement was noticed in the estimation of the mid dosing interval concentrations for the model that took into consideration the estimated bioavailability (models 2a and b). Kwara et al. (2008) noted that efavirenz concentration at steady state was directly related to AUC (of up to 24 h) for individuals on both efavirenz and TB drugs at mid dose and at 24 h. They observed a strong correlation of 0.969 from full PK profile estimates and the work here obtained a correlation of 0.976 of projected estimates. Two main parameters were singled out, that is bioavailability and uptake-volume associated with full absorption in the estimation of absorption. Once absolute oral bioavailability was estimated consequently, the depositing rate constant was taken as 1, a 'parallel' function was used to model the uptake of the drug defined in this work as $x_u(t)$ (Table 11). Efavirenz was being taken up into the systemic circulation at the relative ratio defined by $\frac{A}{V}$ (equation 1.8). The limiting step was the amount of drug available for absorption. The cumulative uptake-volume associated with the uptake of A was shown to consequently follow an asymmetric sigmoid curve and similarly for elimination rate and accumulation of the drug. However, $\frac{A}{V}$ and $\frac{ER_V}{V}$ are constants for any monophasic PK curve.

As far as can be ascertained, this is also the first study which imposed a condition of the existence of an uptake-volume and using the Michaelis-Menten equation to a one compartmental model to relay the process of transportation. The amount of drug cleared per unit time in the dosing interval was noted to be relatively constant for one individual illustrated who had faster absorption (Figures 14 and 15 and Table 11). This could be extended to the whole group. On average in this population, 90% of A (total amount (mass) reaching systemic circulation) was projected to be absorbed in 24 h at steady state (Figure 12, Table 8). The patient who had the quickest transportation in this sample was estimated to have fully absorbed the drug into the systemic circulation in 11 h at steady state (Table 10). This work also highlighted the need to further investigate interpretation of the constants modelled by differential equations and implications (Table 2).

The limitation in this study that could improve estimates includes genetic information on other genotypes linked to efavirenz metabolism such as *CYP3A4, CYP2A6* and possibly transporters (Mukonzo et al., 2009; Kwara et al., 2009; Ritchie et al., 2006). Also, full profiles would ensure that the estimated PK curve is monophasic almost surely. Another improvement on estimates was to model the data above using the value of plasma concentrations in the neighbourhood of 24 h as well (Kwara et al., 2008).

Furthermore, increase in covariate information signifies increase in clusters to be formed which then requires a

Table 11. Estimated absolute amount(s) of the drug in the system and possibilities of its distribution in the patient P.

t	Cumulative uptake volume $V_t(L)$	Amount (mg) cleared per hr (Systemic) $Q_t = C_t - C_{t-1}$	Cumulative mg cleared (Systemic) C_t	$x_u(t)$	Projected (mg) cleared $(D_t - A_t)$	A_t (Systemic)	Total cleared per h (mg) $C^{aII}{}_t - C^{aII}{}_{t-1}$	Cumulative amount cleared (mg) $C^{aII}{}_t$	Amount in systemic (AB_t)	Volume of distribution relative to $x_u(t)$ projected using $(AB_t)/x_u(t)$	Projected plasma Conc. $x(t)$
0	0	-	0	0	0	0		0	0	0	0
1	6.6894	5.0686	5.0686	8.9415	15.302	98.42	20.3706	20.3706	93.3514	10.4403	2.35243
2	12.821	9.3427	14.4113	11.7818	29.328	186.48	23.3687	43.7393	172.069	14.6047	4.33609
3	18.0083	12.8631	27.2744	12.4001	41.1939	264.18	24.729	68.4683	236.906	19.1051	5.96997
4	22.2048	15.1351	42.4095	12.2225	50.7934	321.16	24.7346	93.2029	278.751	22.8064	7.02445
5	25.5407	17.0234	59.4329	11.7724	58.4243	372.96	24.6542	117.857	313.527	26.6325	7.90081
6	28.1911	18.014	77.4469	11.2413	64.487	409.22	24.0768	141.934	331.773	29.5137	8.36061
7	30.3127	18.6869	96.1338	10.6989	69.3402	440.3	23.5401	165.474	344.166	32.1684	8.67291
8	32.0338	19.0584	115.192	10.1697	73.2772	466.2	22.9954	188.469	351.008	34.5151	8.84532
9	33.4478	19.144	134.336	9.6619	76.5117	486.92	22.3785	210.848	352.584	36.4922	8.88503
10	34.6238	18.9584	153.295	9.1777	79.2018	502.46	21.6485	232.496	349.165	38.0449	8.79889
11	35.6	18.7823	172.077	8.7172	82	518	20.927	253.423	345.923	39.6829	8.71718
12	-	17.815	189.892	8.2795	-	-	17.815	271.238	328.108	39.629	8.26825
13	-	16.8976	206.79	7.8637	-	-	16.8976	288.136	311.211	39.5755	7.84243
14	-	16.0273	222.817	7.4688	-	-	16.0273	304.163	295.183	39.5223	7.43855
15	-	15.2019	238.019	7.0936	-	-	15.2019	319.365	279.981	39.4693	7.05546
16	-	14.419	252.438	6.7374	-	-	14.419	333.784	265.562	39.4163	6.69211
17	-	13.6765	266.114	6.399	-	-	13.6765	347.461	251.886	39.3634	6.34746
18	-	12.9721	279.086	6.0776	-	-	12.9721	360.433	238.914	39.3106	6.02057
19	-	12.3041	291.39	5.7723	-	-	12.3041	372.737	226.61	39.2579	5.71051
20	-	11.6704	303.061	5.4824	-	-	11.6704	384.407	214.939	39.2052	5.41642
21	-	11.0694	314.13	5.2071	-	-	11.0694	395.477	203.87	39.1526	5.13747
22	-	10.4993	324.63	4.9455	-	-	10.4993	405.976	193.371	39.1001	4.87289
23	-	9.9586	334.588	4.6971	-	-	9.9586	415.935	183.412	39.0476	4.62194
24	-	9.4457	344.034	4.4612	-	-	9.4457	425.38	173.966	38.9952	4.38391

Table 12. The estimated and projected AUC and AUC_{SS} for efavirenz categorised according to the most significant variable *CYP2B6 G516T* investigated in the separation of observed plasma concentrations in this population sample for the 61 patients.

Genotype		Efavirenz plasma conc. µg/ml median (IQR)	AUC mg h/L median (IQR)	AUC_{ss} mg h/L median (IQR)
CYP2B6 G516T	**GG**	3.32 (1.62, 3.64)	84.16 (57.83, 101.50)	96.77 (65.21, 120.23)
	GT	3.49 (2.81, 6.14)	89.55 (77.51, 127.11)	115.42 (97.53,178.52)
	TT	8.70 (5.01, 11.40)	150.56 (98.91, 180.88)	240.69 (149.00, 297.11)

larger sample size. On validation for estimation of oral bioavailability by the method suggested in this work, an experiment using both intravenous doses and oral doses is required. It is also required to validate what has been estimated in this work with use of data outside this present population.

ACKNOWLEDGEMENTS

The author would like to acknowledge the following persons C. Nhachi, G. Kadzirange and C. Masimirembwa. The following institutions, College of Health Sciences University of Zimbabwe, and AiBST and Novartis Sponsored Pharmacometrics workshops in Africa.

Conflict of Interests

The author(s) have not declared any conflict of interests.

REFERENCES

Aksnes DL, Egge JK (1991). A theoretical model for nutrient uptake in phytoplankton. Mar. Ecol Prog. Ser. 70:65–72.

Almond LM, Hoggard PG, Edirisinghe D, Khoo SH, Back DJ (2005). Intracellular and plasma pharmacokinetics of efavirenz in HIV-infected individuals. J. Antimicrob. Chemother. *56*(4):738–44.

Burger D, van der Heiden I, la Porte C, van der Ende M, Groeneveld P, Richter C, van Schaik R (2006). Interpatient variability in the pharmacokinetics of the HIV non-nucleoside reverse transcriptase inhibitor efavirenz: the effect of gender, race, and CYP2B6 polymorphism. Br. J. Clin. Pharmacol. 61(2):148–54.

Cabrera SE, Santos D, Valverde MP, Domínguez-Gil A, González F, Luna G, MJG (2009). Population Pharmacokinetics of Efavirenz in HIV patients: Influences of CYP2B6 Genotype. Antimicrob. Agents Chemother. 53:2791–2798.

Cristofoletti R, Nair A, Abrahamsson B, Groot DW, Kopp S, Langguth P (2013). Biowaiver Monographs for Immediate Release Solid Oral Dosage Forms: Efavirenz. J. Pharm. Sci. 102(2):318–329.

Csajka C, Marzolini K, Fattinger L, De´costerd A, Fellay J, Telenti A, Biollaz J, Buclin T (2003). Population pharmacokinetics and effects of efavirenz in patients with human immunodeficiency virus infection. Clin. Pharmacol. Ther. 73:20–30

Ette EI, Williams PJ (2007). Pharmacometrics. The Science of Quantitative Pharmacology, (1st ed.). Wiley: Hoboken, New Jersey, USA.

Friedland G, Khoo S, Jack C, Lalloo U (2006). Administration of efavirenz (600 mg/day) with rifampicin results in highly variable levels but excellent clinical outcomes in patients treated for tuberculosis and HIV. J. Antimicrob. Chemother. 58:1299-1302.

Habtewold A, Amogne W, Makonnen E, Yimer G, Riedel KD, Ueda N, Aklillu E (2011). Long-term effect of efavirenz autoinduction on plasma/peripheral blood mononuclear cell drug exposure and CD4 count is influenced by UGT2B7 and CYP2B6 genotypes among HIV patients. J. Antimicrob. Chemother. 66(10):2350-2361.

Jiang F, Desta Z, Shon JH, Yeo CW, Kim HS, Liu KH, Shin JG (2013). Effects of clopidogrel and itraconazole on the disposition of efavirenz and its hydroxyl metabolites: exploration of a novel CYP2B6 phenotyping index. Br. J. Clin. Pharmacol. *75*(1):244–53.

Johnson KA, Goody RS (2011). The original Michaelis constant: translation of the 1913 Michaelis-Menten paper. Biochemistry 50(39):8264–8269.

Kwara A, Lartey M, Sagoe KW, Xexemeku F, Kenu E, Oliver-Commey J, Boima V, Sagoe A, Boamah I, Greenblatt DJ, Court MH (2008). Pharmacokinetics of efavirenz when co-administered with rifampin in TB/HIV co-infected patients: pharmacogenetic effect of CYP2B6 variation. J. Clin. Pharmacol. 48(9):1032–1040.

Kwara A, Lartey M, Sagoe KW, Kenu E, Court MH (2009). CYP2B6, CYP2A6 and UGT2B7 genetic polymorphisms are predictors of efavirenz mid-dose concentration in HIV-infected patients. AIDS, 23(16):2101-2106.

Manosuthi W, Sungkanuparph S, Tantanathip P, Mankatitham W, Lueangniyomkul A, Thongyen S, Ruxrungtham K (2009). Body weight cutoff for daily dosage of efavirenz and 60-week efficacy of efavirenz-based regimen in human immunodeficiency virus and tuberculosis coinfected patients receiving rifampin. Antimicrob. Agents Chemother. 53(10):4545–8.

Mould DR, Upton RN (2013). Basic Concepts in Population Modeling, Simulation, and Model-Based Drug Development—Part 2: Introduction to Pharmacokinetic Modeling Methods. *CPT:* Pharmacometrics Syst. Pharmacol. *2*(4):e38.

Mukonzo JK, Röshammar D, Waako P, Andersson M, Fukasawa T, Milani L, Aklillu E (2009). A novel polymorphism in ABCB1 gene, CYP2B6*6 and sex predict single-dose efavirenz population pharmacokinetics in Ugandans. Br. J. Clin. Pharmacol. 68(5):690–699.

Mukonzo JK, Owen JS, Ogwal-Okeng J, Kuteesa JB, Nanzigu S, Sewankambo N, Thabane L, Gustafsson LL, Ross C, Aklillu E, (2014). Pharmacogenetic-Based Efavirenz Dose modification: Suggestions for an African population and the different CYP2B6 Genotypes. Plos one 9(1):e86919.

Nemaura T, Nhachi C, Masimirembwa C (2012). Impact of gender, weight and CYP2B6 genotype on efavirenz exposure in patients on HIV/AIDS and TB treatment: Implications for individualising therapy. Afr. J. Pharm. Clin. Pharmacol. 6(29):2188-2193.

Nyakutira C, Röshammar D, Chigutsa E, Chonzi P, Ashton M, Nhachi C, Masimirembwa C (2008). High prevalence of the CYP2B6 516G-->T(*6) variant and effect on the population pharmacokinetics of efavirenz in HIV/AIDS outpatients in Zimbabwe. Eur. J. Clin. Pharmacol. 64(4):357–365.

Portier C, Tritscher A, Kohn M, Sewall C, Clark G, Edler L, Lucier G (1993). Ligand/receptor binding for 2,3,7,8-TCDD: implications for risk assessment. Fundam. Appl. Toxicol. 20(1):48–56.

Pedral-Sampaio DB, Alves CR, Netto EM, Brites C, Oliveira AS, Badaro R (2004). Efficacy and safety of Efavirenz in HIV patients on Rifampin for tuberculosis. Braz. J. Infect. Dis. 8(3):211–216.

Rekić D, Röshammar D, Mukonzo J, Ashton M (2011). *In silico* prediction of efavirenz and rifampicin drug-drug interaction considering weight and CYP2B6 phenotype. Brit. J. Clin. Pharmacol 71(4):536–543.

Ritchie MD, Haas DW, Motsinger AA, Donahue JP, Erdem H, Raffanti S, Sterling TR (2006). Drug transporter and metabolizing enzyme gene variants and nonnucleoside reverse-transcriptase inhibitor hepatotoxicity. Clin. Infect. Dis. 43(6):779–782.

Ribaudo HJ, Haas DW, Tierney C, Kim RB, Wilkinson GR, Gulick RM, Acosta EP (2006). Pharmacogenetics of plasma efavirenz exposure after treatment discontinuation: an Adult AIDS Clinical Trials Group Study. Clin. Infect. Dis. 42(3):401–407.

Ribaudo HJ, Liu H, Schwab M, Schaeffeler E, Motsinger-reif AA, Ritchie MD, Haas DW (2011). Effect of CYP2B6, ABCB1, and CYP3A5 polymorphisms on efavirenz pharmacokinetics and treatment response: an AIDS Clinical Trials Group study. J. Infect. Dis. 202(5):717–722.

Sánchez A, Cabrera S, Santos D, Valverde MP, Fuertes A, Domínguez-Gil A, García MJ (2011). Population pharmacokinetic/ pharmacogenetic model for optimization of efavirenz therapy in Caucasian HIV-infected patients. Antimicrob. Agents Chemother. 55(11):5314–5324.

Siccardi M, Almond L, Schipani A, Csajka C, Marzolini C, Wyen C, Back D (2012). Pharmacokinetic and pharmacodynamic analysis of efavirenz dose reduction using an in vitro-*in vivo* extrapolation model. Clin. Pharmacol. Ther. *92*(4):494–502.

Smith PF, DiCenzo R, Morse GD (2001). Clinical uses of non-nucleoside reverse transcriptase inhibitors. Clin. Pharmacokinet. 10(4):217–229.

Toutain PL, Bousquet-Mélou A (2004a). Plasma terminal half-life. J. Vet. Pharmacol. Ther. 27(6):427–439.

Toutain PL, Bousquet-Mélou A (2004b). Volumes of distribution. J. Vet. Pharmacol. Ther. 27(6):441–453.

Van Luin M, Gras L, Richter C, Van Der Ende ME, Prins JM, De Wolf F,

Wit FW (2009). Efavirenz dose reduction is safe in patients with high plasma concentrations and may prevent efavirenz discontinuations. J. Acquir. Immune Defic. Syndr. 52:240–245.

Yilmaz A, Watson V, Dickinson L, Back D (2012). Efavirenz pharmacokinetics in cerebrospinal fluid and plasma over a 24-hour dosing interval. Antimicrob. Agents Chemother. 56(9):4583–4585.